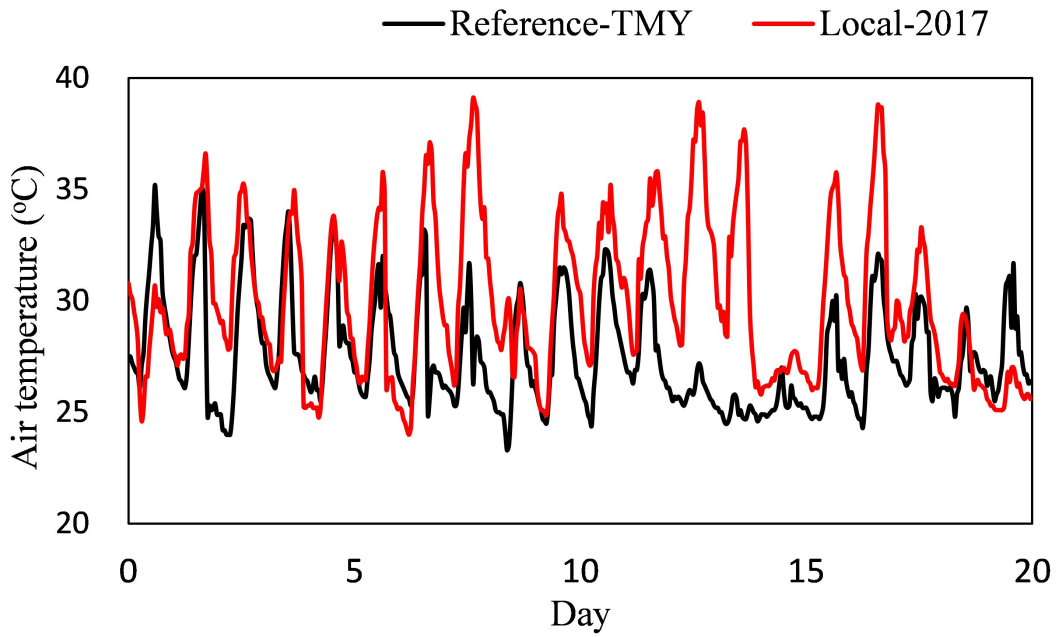


Short C.A., Song J., Mottet L., Chen S., Wu J., Ge J. (2018). Challenges in the low carbon adaptation of China's apartment towers. *Building Research & Information*.

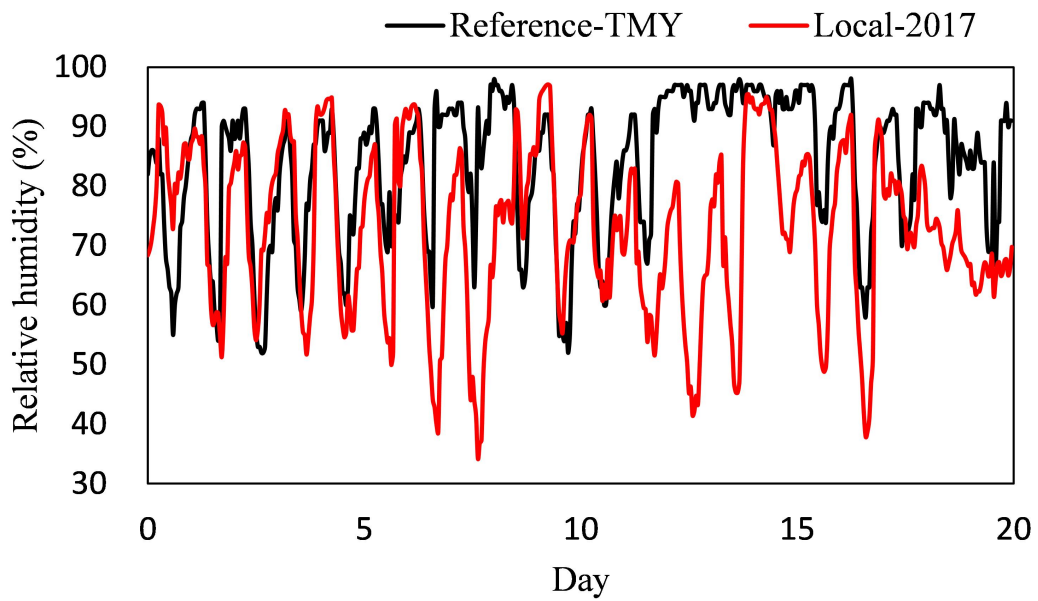
## Supplemental data

**Table S1.** Liubo building: construction materials listed by element.

Building envelope	Construction	Thickness (mm)	Conductivity ( $\text{Wm}^{-1}\text{K}^{-1}$ )	Density ( $\text{kgm}^{-3}$ )	Specific heat ( $\text{Jkg}^{-1}\text{K}^{-1}$ )
Exterior wall	Bloated perlite board (Outer layer)	35	0.072	300	837
	Fire-proof Alkali Resistant Glass Fibre Mesh	6	0.3	2.5	800
	Cement mortar	20	0.93	1800	1050
	Reinforced Concrete	300	1.74	2500	2500
	Mixed mortar	20	0.9	1500	1000
Interior Wall	Cement mortar	20	0.93	1800	1050
	Reinforced Concrete	200	1.74	2500	2500
	Cement mortar	20	0.93	1800	1050
Ceiling	Cement mortar	20	0.93	1800	1050
	Reinforced Concrete	120	1.74	2500	2500
	Cement mortar	20	0.93	1800	1050
Floor	Wood floor (Upper Layer)	20	0.115	800	1380
	Cement mortar	20	0.93	1800	1050
	Reinforced Concrete	120	1.74	2500	2500
	Cement mortar	20	0.93	1800	1050



(a)



(b)

**Figure S1.** a) Typical Meteorological Year (TMY) Dry Bulb Temperature and b) TMY Relative Humidity data for the month of August set against Local-2017 data collected in August 2017 from the Local weather station adjacent to the Liubo building.

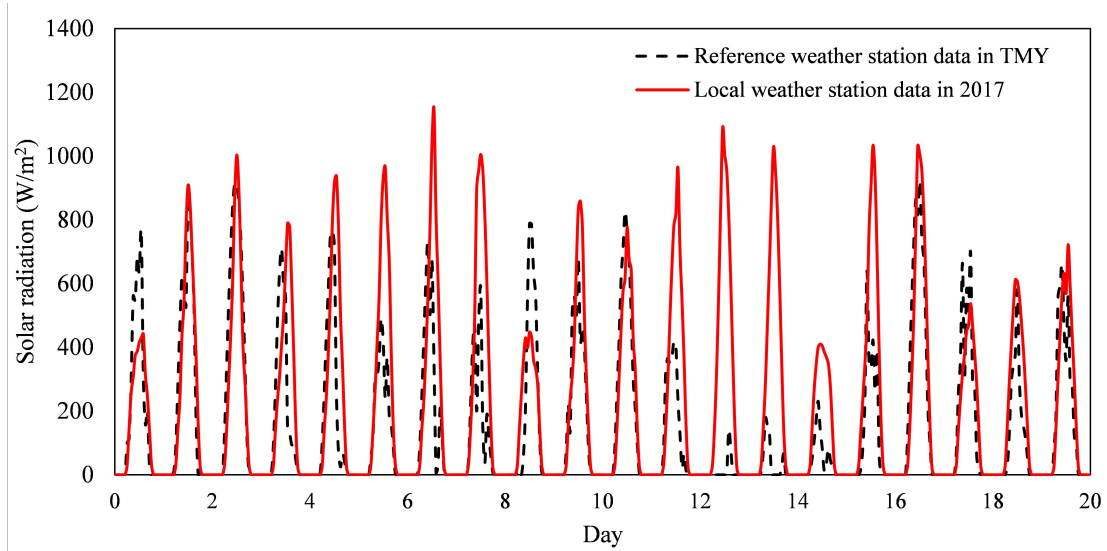
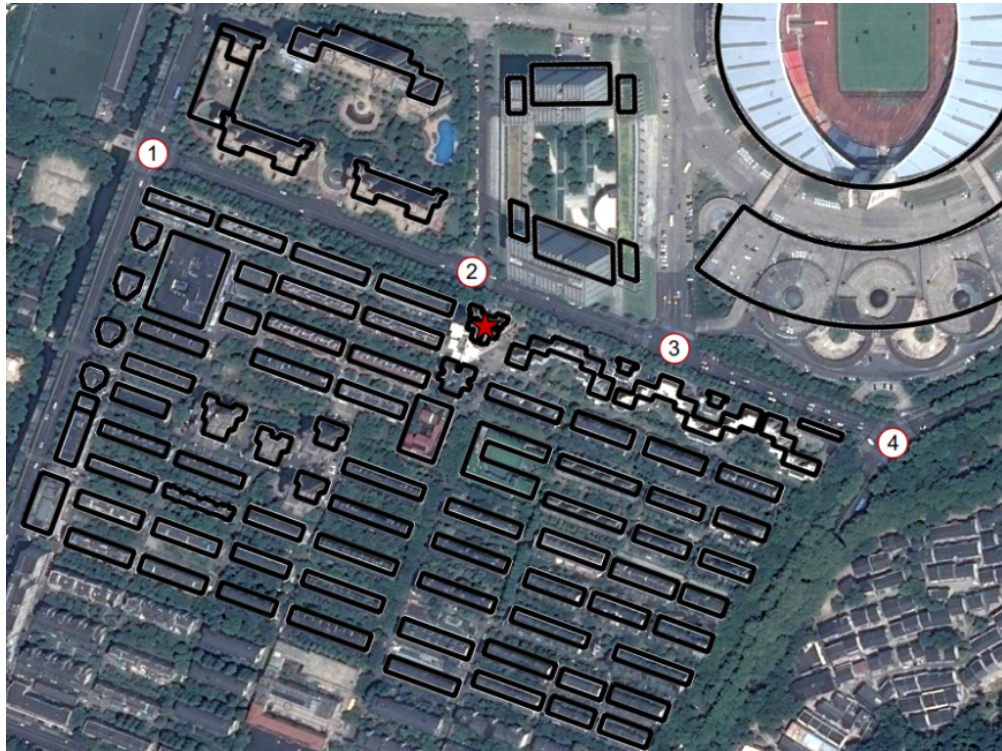
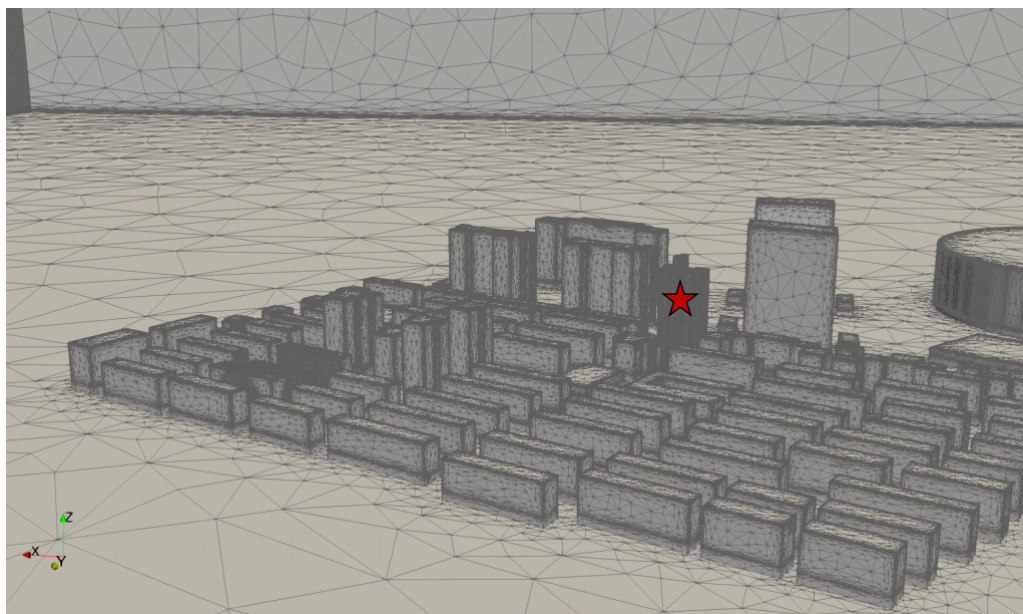


**Figure S2.** Measured solar radiation at the Local weather station between August 12th and 31st 2017 compared with TMY data for the same notional summer period.



(a)



(b)

**Figure S3.** a) Area of interest used in CFD simulations including 95 buildings within the Zhejiang University in Hangzhou. Black lines depict the footprints of buildings including in the simulations. The numbers 1, 2, 3 and 4 correspond to the locations of the main crossroads, sources of pollution and b) Initial unstructured mesh. The red star shows the location of the Liubo building.

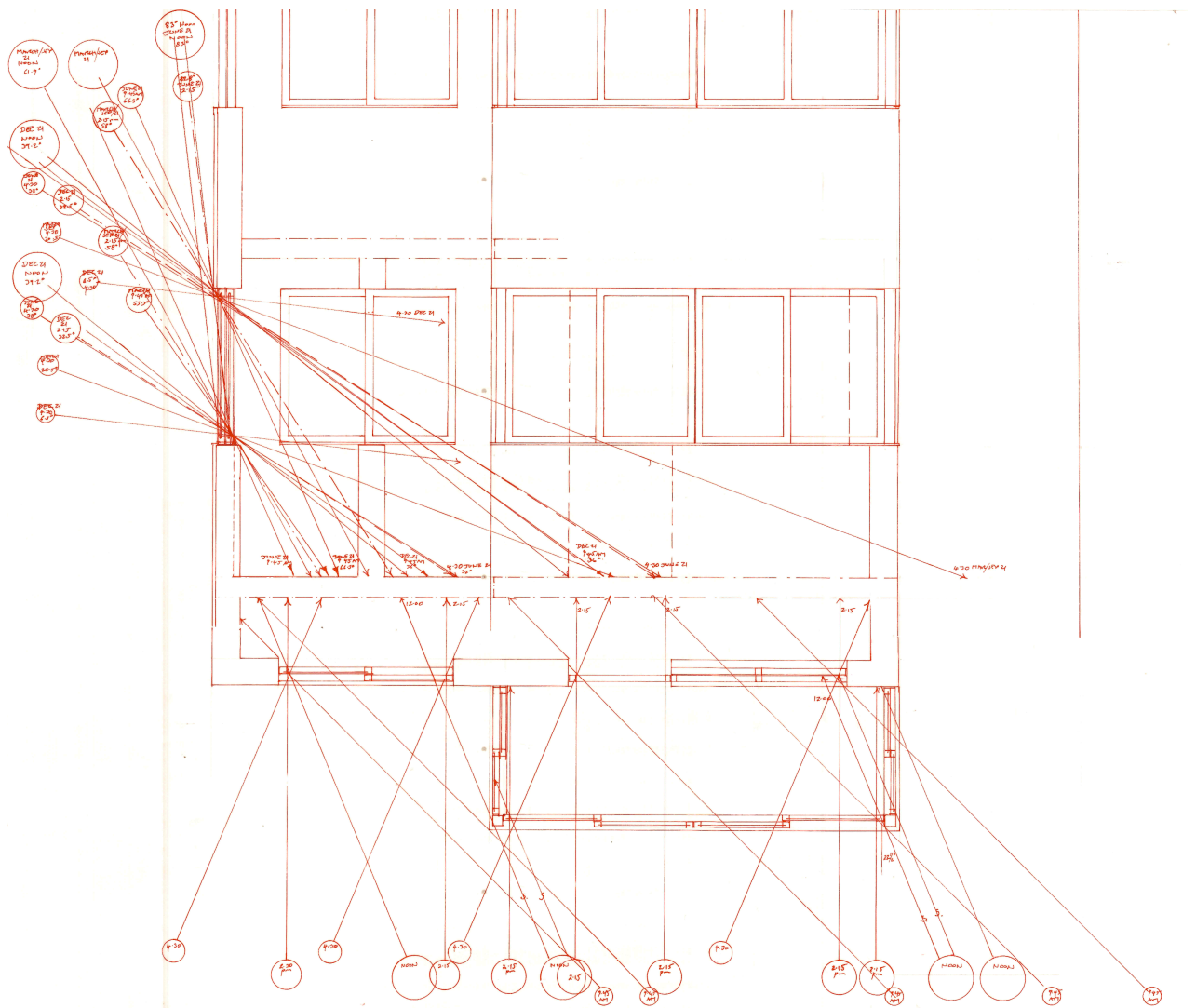


**Figure S4**, Solar geometries at the south-south-west facing balcony elevation of Flat 4 at December, March, September and June.

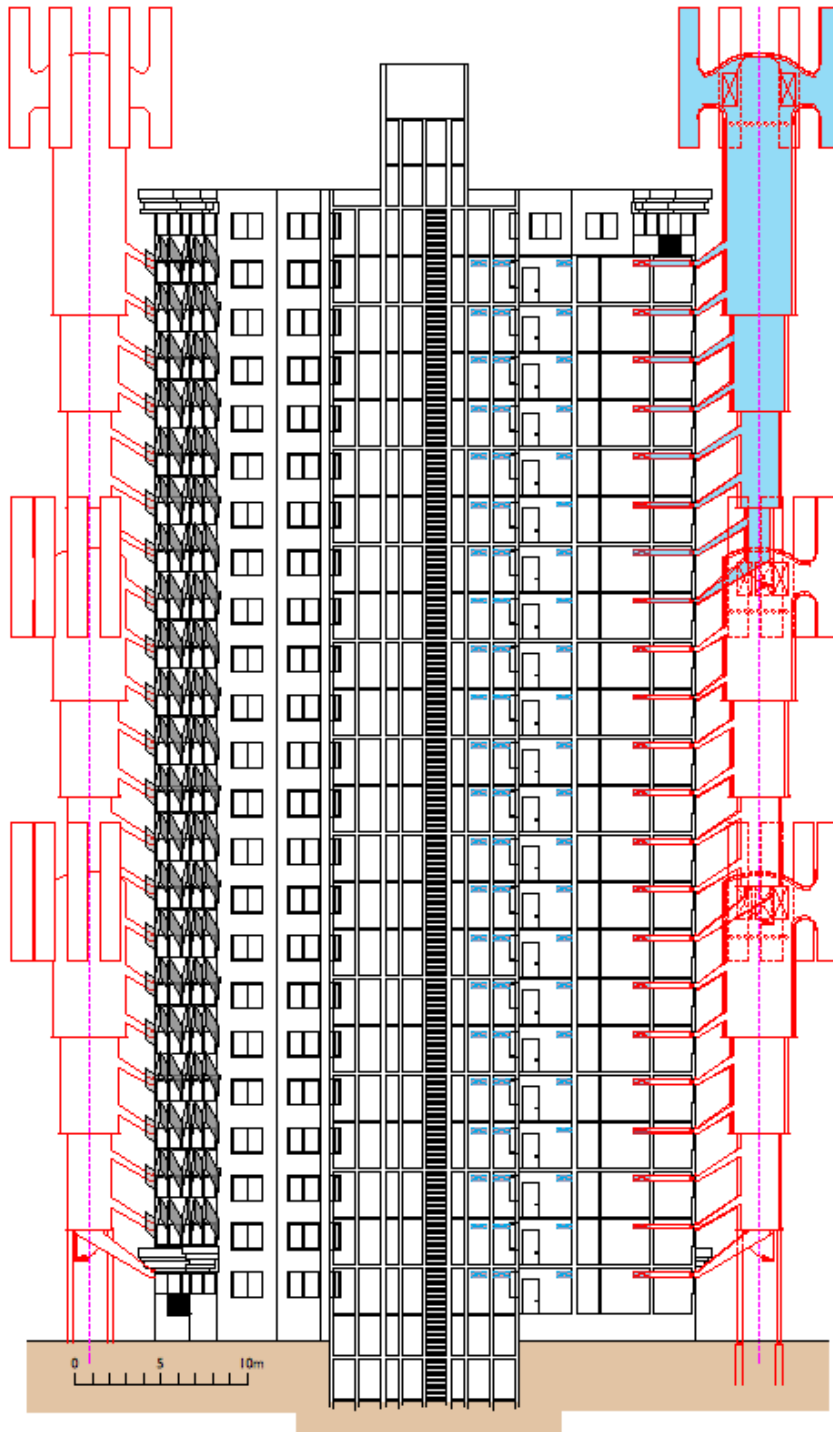


**Figure S5.** During periods in which internal temperatures are likely to exceed the maximum prescribed by the regional adaptive comfort standard flow is reversed as Passive Dwindraught Cooling is induced within the stacks by cooling batteries located below the cross pot H-Pot termination to develop downward flow back into the flats, flowing out through what are the intake ducts in less hot conditions.

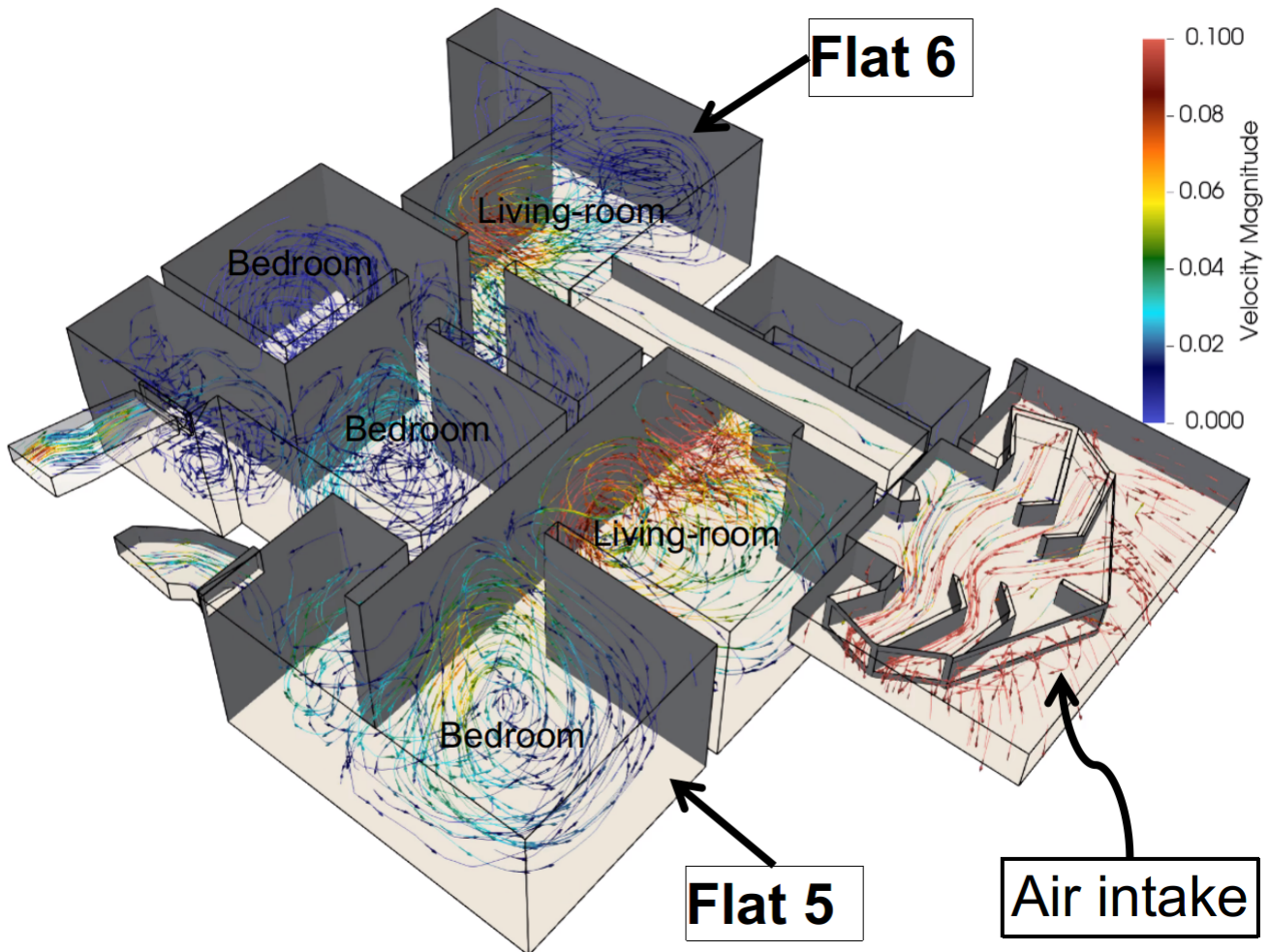
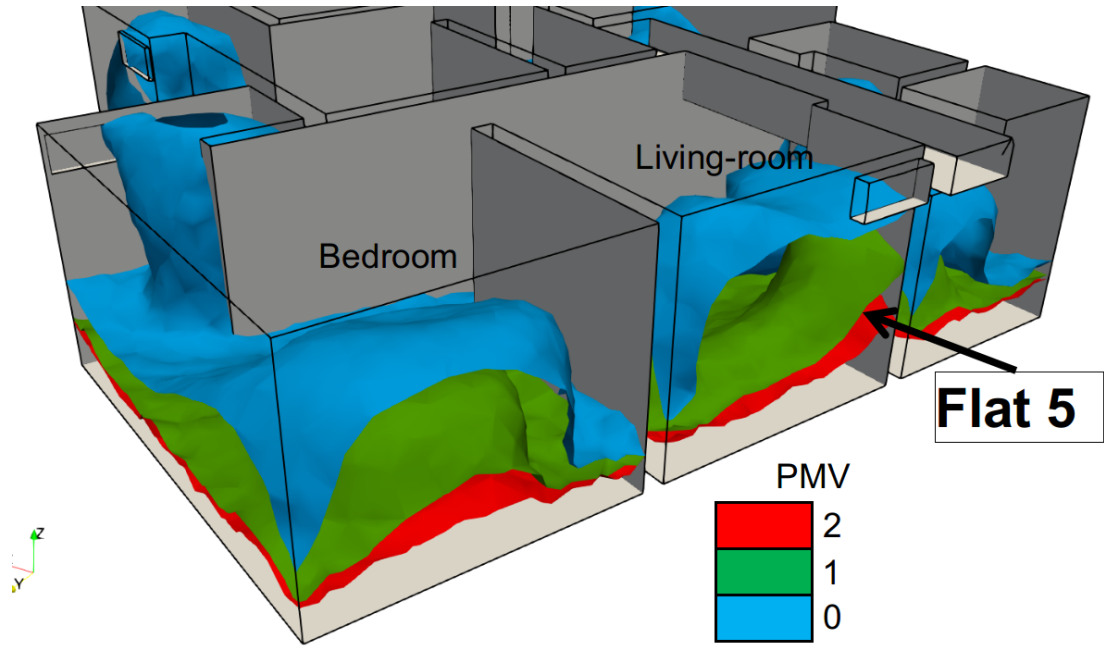
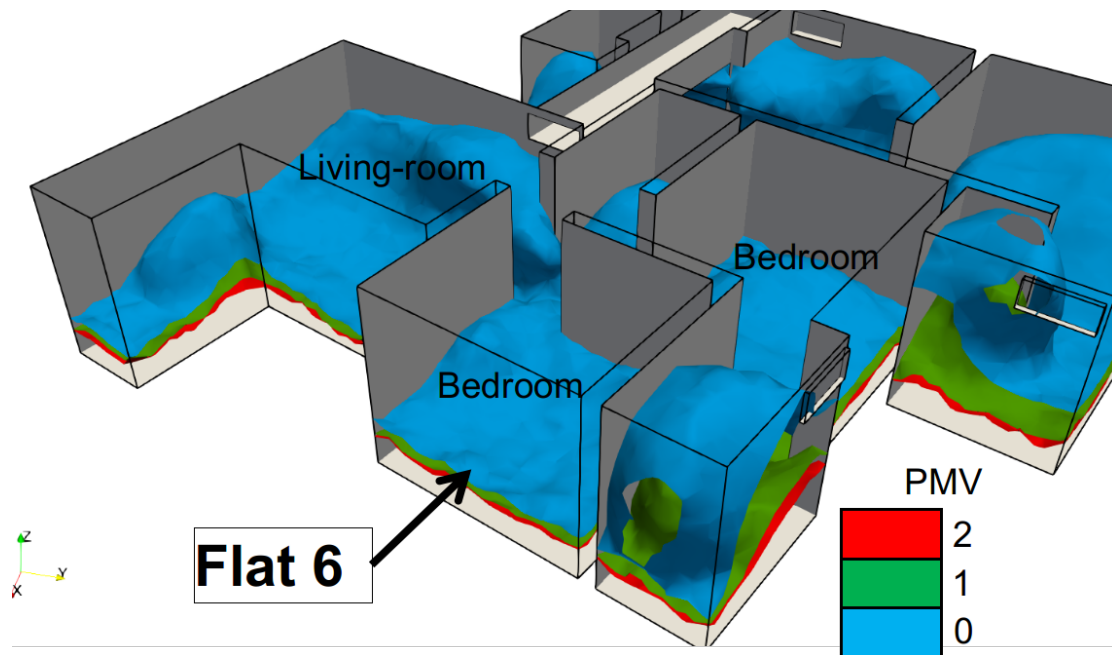


**Figure S6.** “Reversed” air flow periodically occurring within Flat 5 and 6 for a northerly wind. Time is equal to 610 seconds on this screen-shot.



(a)



(b)

**Figure S7.** Predicted Mean Vote (PMV) using Fanger's (1970) theory in a) the Flat 5 and b) the Flat 6 for a northerly wind.